

## Indium-induced triple-period atomic wires on a vicinal Si(111) surface: In/Si(557)

I Song<sup>1,2</sup>, D-H Oh<sup>3</sup>, J H Nam<sup>1,2</sup>, M K Kim<sup>1,2</sup>, C Jeon<sup>2</sup>,  
C-Y Park<sup>1,2,3,4</sup>, S H Woo<sup>5</sup> and J R Ahn<sup>1,2,3,4,6</sup>

<sup>1</sup> BK21 Physics Research Division, Sungkyunkwan University,  
Suwon 440-746, Republic of Korea

<sup>2</sup> Center for Nanotubes and Nanostructured Composites (CNNC),  
Sungkyunkwan University, Suwon 440-746, Republic of Korea

<sup>3</sup> Institute of Basic Science, Sungkyunkwan University,  
Suwon 440-746, Republic of Korea

<sup>4</sup> SKKU Advanced Institute of Technology (SAINT), Sungkyunkwan  
University, Suwon 440-746, Republic of Korea

<sup>5</sup> College of Pharmacy, Chungnam National University,  
Daejeon 305-764, Republic of Korea

E-mail: [ohdh@skku.edu](mailto:ohdh@skku.edu), [cypark@skku.edu](mailto:cypark@skku.edu) and [jrahn@skku.edu](mailto:jrahn@skku.edu)

*New Journal of Physics* **11** (2009) 063034 (11pp)

Received 25 March 2009

Published 16 June 2009

Online at <http://www.njp.org/>

doi:10.1088/1367-2630/11/6/063034

**Abstract.** An indium-induced one-dimensional (1D) surface reconstruction on a Si(557) surface was studied by the combined approach of scanning tunneling microscopy (STM) and first principles calculations. Low-energy electron diffraction revealed a  $(1 \times 3)$  phase with a triple-period along the step edge direction, which was also confirmed by STM. The STM images showed that the 1D structure consists of two atomic chains. One is located on the terrace and consists of triple-period bright protrusions. The other shows a weak  $\times 3$  modulation at the step edge. Five atomic structure models based on the In adatom of a In/Si(111)- $\sqrt{3} \times \sqrt{3}$  surface were considered to figure out the underlying structure of the STM images of the In/Si(557)- $1 \times 3$  surface. Interestingly, a heterogeneous In–Si adatom chain model reproduced most of the features of STM images and was the most stable energetically at a wide range of In chemical potential.

<sup>6</sup> Author to whom any correspondence should be addressed.

**Contents**

<b>1. Introduction</b>	<b>2</b>
<b>2. Method</b>	<b>3</b>
<b>3. Results and discussion</b>	<b>3</b>
3.1. LEED and STM experiments . . . . .	3
3.2. Atomic structure models . . . . .	5
<b>4. Conclusions</b>	<b>9</b>
<b>Acknowledgments</b>	<b>10</b>
<b>References</b>	<b>10</b>

**1. Introduction**

Atomic wires have become a subject of intensive research after the findings of various exotic one-dimensional (1D) phenomena such as Peierls instability. At the early stage, atomic wires grown on a Si(111) surface prompted the studies of 1D electron systems. The most intensively studied atomic wires on a Si(111) surface have been an In zigzag chain on an In/Si(111)- $4 \times 1$  surface [1]–[6], an Si double honeycomb chain on an Au/Si(111)- $5 \times 2$  surface [7]–[11] and an Si honeycomb chain channel on a metal (Na, Li, Ag, Mg)/Si(111)- $3 \times 1$  surface [12, 13]. Peierls instability [1] and the gap openings of multiple metallic bands [4] have been observed in the In zigzag chain. The Si double honeycomb chain has allowed the observations of the transition from 2D to 1D states [7], an inhomogeneous quantum wire [9] and a hopping domain wall [11]. The Si honeycomb chain channel was used to produce a 1D Mott–Hubbard insulator [13].

Recently, vicinal Si(111) surfaces have proven to be more efficient in producing atomic wires than an Si(111) surface. A few nanometer scale terrace size of vicinal Si(111) surfaces acts as a 1D template for metal-induced atomic wire growth. In addition, their step edges could weaken the electronic and atomic correlations between atomic wires located on neighboring terraces. This could make atomic wires on vicinal Si(111) surfaces closer to a 1D structure. In particular, the different physical properties of Au-induced atomic wires on Si(557) and Si(553) surfaces from the Au/Si(111)- $5 \times 2$  surface have ignited research into the vicinal Si(111) surfaces [14]–[21]. Different temperature-dependent transitions of two proximal bands [15] and a 1D plasmon [16] were observed on the Au/Si(557) surface. In addition, the coexistence of two different Peierls instabilities [18, 20] and 1D spin–orbit split bands [21] were found on the Au/Si(553) surface.

Quite recently, the studies of the Au/Si(557) and Au/Si(553) surfaces were extended to Pb/Si(557) surfaces to investigate other 1D phenomena such as switching between 1D and 2D in conductance and the strong lateral coupling of Pb nanowires [22]–[24]. The previous studies of the metal/vicinal Si(111) surfaces suggest that counterparts on a vicinal Si(111) surface of metal-induced phases on an Si(111) surface provide an opportunity in exploring a new 1D phenomenon, which has not been found on metal-induced Si(111) surfaces. In this study, a counterpart on a vicinal Si(111) surface of an In/Si(111) surface has been explored to study how the change of the terrace width affects In-induced surface reconstructions on a Si(111) surface. On a In/Si(111)- $\sqrt{3} \times \sqrt{3}$  surface with low In coverage, a 2D In adatom array is stable.

In contrast, a 1D heterogeneous In–Si adatom chain structure was found on an In/Si(557)- $1 \times 3$  surface with low In coverage.

## 2. Method

The experiments were performed in an ultrahigh vacuum chamber equipped with commercial variable-temperature scanning tunneling microscopy (STM) (Omicron, Germany) and low-energy electron diffraction (LEED). An n-type phosphorus-doped Si(557) wafer with resistivity of 1–10  $\Omega\text{cm}$  was used. The Si(557) substrate ( $9.45^\circ$  offcut from the [111] orientation) was cleaned thermally [25, 26]. In was deposited by heating resistively a tungsten wire wrapping an In rod. In coverage of the In/Si(557)- $1 \times 3$  surface was measured from the relative integrated intensity ( $I_{1 \times 3}/I_{1 \times 4}$ ) of an In  $4d$  core-level spectrum to that of the In/Si(111)- $4 \times 1$  surface with In coverage of 1 monolayer (ML) after subtracting backgrounds. Here, the two In  $4d$  spectra were measured under the same experimental conditions such as photon energy and emission angle.  $I_{1 \times 3}/I_{1 \times 4}$  was  $0.12 \pm 0.01$ , which suggests that In coverage of the In/Si(557)- $1 \times 3$  surface is  $0.12 \pm 0.01$  ML. However, both the In/Si(557)- $1 \times 3$  and In/Si(111)- $4 \times 1$  surfaces form within a finite range of In coverage. The error range of In coverage, thus, should be larger than that calculated by the mathematical analysis. This leads to the conclusion that In coverage of the In/Si(557)- $1 \times 3$  surface is  $0.12 \pm 0.07$  ML.

First principle calculations were performed using VASP [27], which is a plane-wave-pseudopotential code based on density functional theory. The electron–electron and electron–ion potentials were described by a local density approximation [28] and a projected augmented wave method [29], respectively. The electronic wave functions were expanded by plane waves up to a kinetic energy cutoff of 250 eV. A slab geometry in an orthorhombic unit cell was used to describe the Si(557) surface, where the surface area was  $19.2 \times 3.84 \text{ \AA}^2$  for the ( $1 \times 1$ ) unit cell. This unit cell contains three Si bilayers, where Si atoms at the bottom were saturated with hydrogen. A vacuum region of approximately 10  $\text{\AA}$  was used.  $\Gamma$  point was sampled in the surface Brillouin zone. A combination of quenched dynamics and quasi-Newtonian methods was used for structure relaxation, where the criterion of force was  $2.0 \times 10^{-2} \text{ eV \AA}^{-1}$ . A simulated STM image was calculated using the method proposed by Tersoff and Hamann [30].

## 3. Results and discussion

### 3.1. LEED and STM experiments

LEED patterns were obtained with increasing annealing temperature after room temperature (RT) In adsorption above 1 ML. The  $\times 7$  LEED pattern of a clean Si(557) surface was changed to a diffuse  $\times 1$  LEED pattern after the RT In adsorption. A  $\times 3$  LEED pattern was observed at the annealing temperature ranging from 480 to 530  $^\circ\text{C}$ , as shown in figure 1, where the optimal annealing temperature was found to be 530  $^\circ\text{C}$ . Above 530  $^\circ\text{C}$ , the  $\times 7$  LEED pattern reappeared, which indicates a coverage-dependent phase transition from the In/Si(557) surface to the clean Si(557) surface. The  $\times 3$  periodicity along the step edge direction was also confirmed by STM, as shown in figure 1. The empty-state STM image shows that the ( $1 \times 3$ ) phase consists of triple-period protrusion chains along the step edge direction. In contrast, the protrusions are not coherent across the step edge direction, as expected from the streak  $\times 3$  LEED pattern.

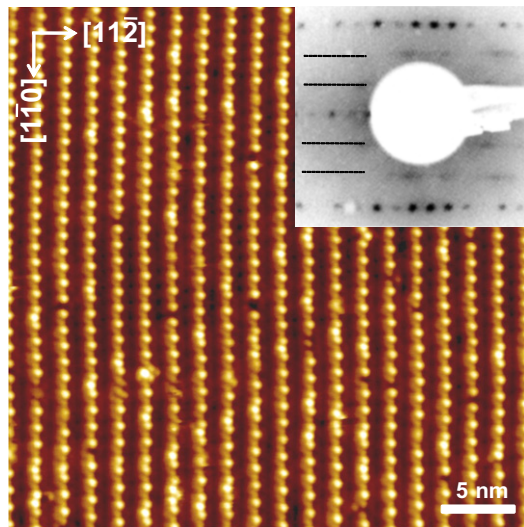


**Figure 1.** The empty-state STM image ( $V_s = +1.2$  V) of the In/Si(557)- $1 \times 3$  surface. The inset is the LEED pattern corresponding to the STM image. The crystallographic directions of experimental and simulated STM images in other figures are the same as those in this figure.

The anisotropic coherent length suggests that the underlying atomic chains are close to a 1D structure. The terrace width of the ( $1 \times 3$ ) phase was estimated to be 1.92 nm from the LEED pattern by measuring the distance between LEED spots along the  $[11\bar{2}]$  direction. The terrace width was consistent with that measured from the STM image. This leads to the conclusion that the In/Si(557)- $1 \times 3$  surface has the same terrace width as the bulk-terminated Si(557)- $1 \times 1$  structure [15].

A dual  $V_s$  STM image was also acquired, as shown in figure 2(a), in order to connect the registries of filled- and empty-state STM images, where  $V_s$  was changed from +1.2 to  $-1.2$  V in the middle of the STM image. The filled-state STM image consists of one bright straight chain ( $\alpha$ ) and two bright protrusion chains ( $\alpha_L$  and  $\alpha_R$ ). The  $\alpha_L$  and  $\alpha_R$  chains have  $\times 3$  periodicity along the step edge direction, while the  $\alpha$  chain has  $\times 1$  periodicity. The triple-period bright protrusion chain ( $\beta$ ) observed in the empty-state STM image is separated by 0.6 nm from the  $\alpha$  chain, whereas the  $\alpha_L$  and  $\alpha_R$  chains are separated by 0.7 and 0.6 nm from the  $\alpha$  chain, respectively.

The chains observed in the dual  $V_s$  STM image were further studied by extending  $V_s$ . Figure 2(b) shows  $V_s$ -dependent STM images ranging from  $-1.8$  to  $+1.8$  V. In the filled-state STM images, the  $\alpha$  chain reveals the most interesting  $V_s$  dependence. The  $\alpha$  chain, which has  $\times 1$  periodicity at  $V_s = -1.2$  V, shows a weak  $\times 3$  periodic modulation at lower  $V_s$ . The modulation indicates that the  $\alpha$  chain also has the same  $\times 3$  periodicity as the other chains. The  $\alpha_L$  and  $\alpha_R$  chains appear equivalent at  $V_s = -1.2$  V. However, the  $\alpha_L$  chain becomes brighter at higher  $V_s$ , whereas the  $\alpha_R$  chain is invariant. The different  $V_s$  dependence suggests that the  $\alpha_L$  and  $\alpha_R$  chains arise from different atomic structures. On the other hand, in the empty-state STM images, distinctive  $V_s$  dependence was observed on the  $\beta$  chain. The  $\beta$  chain is built up of bright protrusions with  $\times 3$  periodicity at high  $V_s$ . In contrast, at lower  $V_s$ , additional bright protrusions become visible resulting in a zigzag chain.

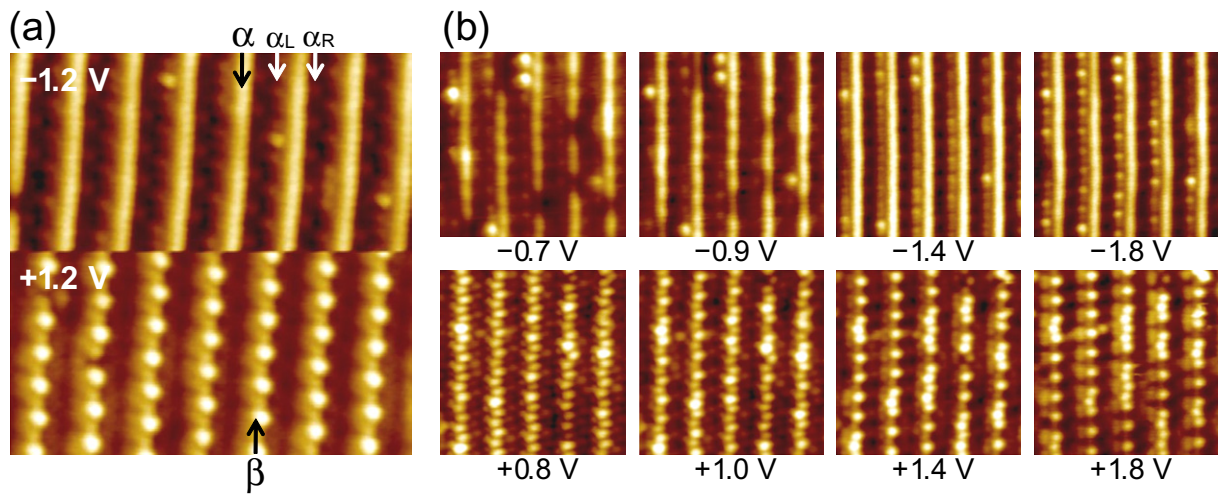


**Figure 2.** The detailed  $V_s$  dependence of the STM images of the In/Si(557)-1  $\times$  3 surface. (a) An STM image with a dual  $V_s$  of  $\pm 1.2$  V, where  $V_s$  was switched from +1.2 to  $-1.2$  V in the middle of the image.  $\alpha$ ,  $\alpha_L$  and  $\alpha_R$  in (a) denote three chains in the filled-state STM image and  $\beta$  denotes a single chain in the empty-state STM image. (b) STM images with various  $V_s$  ranging from  $-1.8$  to  $+1.8$  V. The  $V_s$  of each STM image is written at the bottom.

### 3.2. Atomic structure models

In the STM images of the Au/Si(557)-1  $\times$  2 surface, two atomic chains with  $\times 1$  and  $\times 2$  periodicity along the step edge direction have been observed [15, 31, 32]. The  $\times 1$  chain originates from a Si step edge structure, whereas the  $\times 2$  chain arises from an Si adatom on a terrace [32]. The  $\times 1$  and  $\times 2$  chains are quite similar to the  $\alpha$  and  $\beta$  chains of the In/Si(557)-1  $\times$  3 surface, respectively [15, 31, 32]. In addition, both the In/Si(557)-1  $\times$  3 and Au/Si(557)-1  $\times$  2 surfaces have the same terrace width as the bulk-terminated Si(557)-1  $\times$  1 structure. The similarities suggest that the In/Si(557)-1  $\times$  3 surface has an atomic structure analogy to the Au/Si(557)-1  $\times$  2 surface.

Another clue for understanding the atomic structure of the In/Si(557)-1  $\times$  3 surface is a strong atomic structure resemblance between metal/vicinal Si(111) and metal/Si(111) surfaces. For example, Au-induced surface reconstructions on a Si(557) surface result in (1  $\times$  2) and ( $\sqrt{3} \times \sqrt{3}$ ) phases with increasing Au coverage [15]. The two surfaces have similar Au-Si bonds to Au/Si(111)-5  $\times$  2 and  $-\sqrt{3} \times \sqrt{3}$  surfaces, respectively [33]. Therefore, the well-established atomic structure models of the In/Si(111) surfaces need to be referred in order to develop a more reasonable approach to the atomic structure model of the In/Si(557)-1  $\times$  3 surface. Various surface reconstructions have been found on the In/Si(111) surfaces: ( $\sqrt{3} \times \sqrt{3}$ ), ( $\sqrt{31} \times \sqrt{31}$ ), and (4  $\times$  1) surfaces are produced sequentially with increasing In coverage up to 1 ML [34]. Among the phases, the In/Si(111)- $\sqrt{3} \times \sqrt{3}$  surface has the lowest In coverage of 1/3 ML and is optimized at the annealing temperature of 550  $^\circ$ C [34]–[36]. The In/Si(557)-1  $\times$  3 surface also has the lowest In coverage on the In/Si(557) surface and is optimized at annealing temperature of 530  $^\circ$ C. The resemblance suggests that the In/Si(557)-1  $\times$  3 surface could have a similar In-Si bond to the In/Si(111)- $\sqrt{3} \times \sqrt{3}$  surface. On the

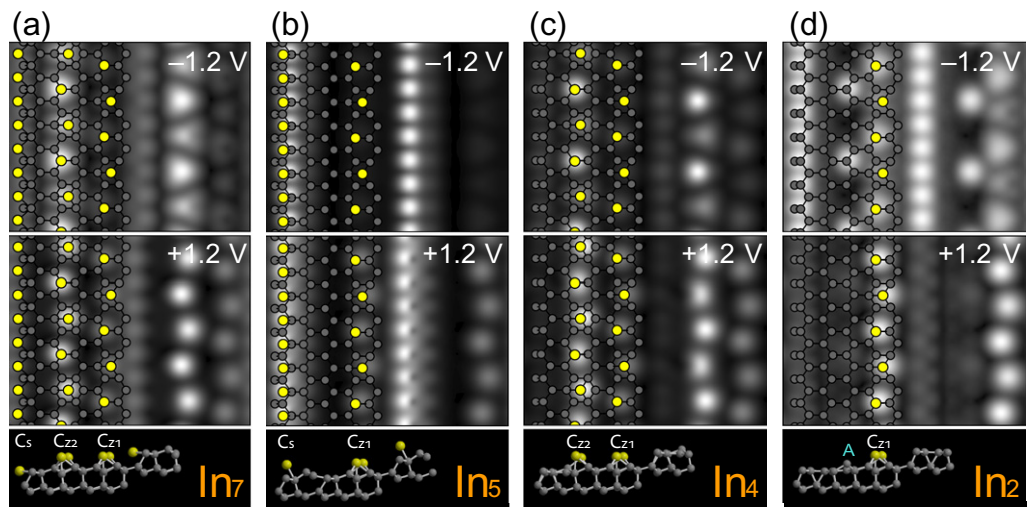


**Figure 3.** The simulated filled- and empty-state STM images with  $V_s = -1.2$  and  $+1.2$  V, respectively, of the (a)  $\text{In}_7$ , (b)  $\text{In}_5$ , (c)  $\text{In}_4$  and (d)  $\text{In}_2$  models. Atomic structure models are drawn at the bottom. The yellow and gray solid circles denote In and Si atoms, respectively. The three In chains are denoted by  $C_{z1}$ ,  $C_{z2}$  and  $C_s$  and the raised Si atom in (d) is denoted by A.

$\text{In}/\text{Si}(111)-\sqrt{3} \times \sqrt{3}$  surface, In adatoms are located at threefold sites saturating the Si dangling bonds of the bulk-terminated  $\text{Si}(111)-1 \times 1$  structure, where the In adatom prefers energetically a  $T_4$  site between the two threefold sites  $T_4$  and  $H_3$  [37, 38].

For these reasons, the bulk-terminated  $\text{Si}(557)-1 \times 1$  and  $\text{In}/\text{Si}(111)-\sqrt{3} \times \sqrt{3}$  structures were referred in constructing the atomic structure models of the  $\text{In}/\text{Si}(557)-1 \times 3$  surface. Firstly, the bulk-terminated  $\text{Si}(557)-1 \times 1$  structure was used as a cornerstone of the atomic structure models of the  $\text{In}/\text{Si}(557)-1 \times 3$  surface. Secondly, an In adatom on the  $\text{In}/\text{Si}(111)-\sqrt{3} \times \sqrt{3}$  surface was imaged as a bright protrusion in an empty-state STM image [36, 39]. Hence, an In adatom on the  $\text{Si}(557)$  surface is expected to appear like a bright protrusion in an empty-state STM image. The  $\beta$  chain in the empty-state STM images is made out of zigzag bright protrusions. This suggests that an In adatom is located at the  $\beta$  chain. The restriction leaves four threefold sites (two  $H_3$  and two  $T_4$  sites) on the terrace as the adsorption sites of In adatoms, which results in two zigzag In chains along the step edge direction. It is also considered that In atoms could be adsorbed at the step edge forming a straight chain. Figure 3 shows four atomic structure models based on the three In chains. Two zigzag In adatom chains ( $C_{z1}$  and  $C_{z2}$ ) are on the terrace, where the alternative arrangement of In adatoms located at the  $T_4$  and  $H_3$  sites produces the  $\times 3$  periodicity along the step edge direction. One linear chain with  $\times 1$  periodicity ( $C_s$ ) is located at the step edge. The  $\text{In}_7$  model consists of the  $C_s$ ,  $C_{z1}$  and  $C_{z2}$  chains, while the  $C_s$  chain is removed in the  $\text{In}_4$  model. In comparison to the  $\text{In}_7$  and  $\text{In}_4$  models, the  $C_{z2}$  chain is excluded in the  $\text{In}_5$  and  $\text{In}_2$  models. Here, In coverage of the  $\text{In}_7$ ,  $\text{In}_5$ ,  $\text{In}_4$  and  $\text{In}_2$  models is 0.41, 0.29, 0.24 and 0.12 ML, respectively. In coverage of the  $\text{In}_7$  and  $\text{In}_5$  models is out of the experimental In coverage, but the  $\text{In}_7$  and  $\text{In}_5$  models were also considered for a schematic theoretical analysis.

Figure 3 shows simulated STM images with  $V_s$  of  $\pm 1.2$  V of the four atomic structure models, which were calculated after *ab initio* total energy minimizations. Firstly, the In<sub>7</sub> and In<sub>4</sub> models produce a bright zigzag chain on the C<sub>z2</sub> chain on both the filled- and empty-state STM images, as shown in figures 3(a) and (c). However, the simulated STM images do not reproduce the  $\alpha$  and  $\beta$  chains shown in the experimental STM images. Secondly, both the simulated filled- and empty-state STM images of the In<sub>5</sub> model in figure 3(b) show a bright line on the C<sub>s</sub> chain, which also conflicts with the experimental STM images. Thirdly, the simulated filled-state STM image of the In<sub>2</sub> model in figure 3(d) produces a bright straight chain on the Si step edge. The bright straight chain is consistent with the  $\alpha$  chain in the experimental STM images. Moreover, the zigzag structure of the  $\beta$  chain in the experimental STM images is also reproduced by the C<sub>z1</sub> chain in the simulated STM image. Therefore, the In<sub>2</sub> model is the most reliable among the four candidates examined. There are some interesting features in the simulated STM images of the In<sub>2</sub> model. The zigzag In adatom chain with  $\times 3$  periodicity induces structure modulations on the neighboring Si structures. Every third atom of the neighboring Si chain is raised by approximately 1 Å, where the raised Si atom is denoted by A. This results in a bright protrusion chain with  $\times 3$  periodicity in the simulated filled-state STM image. The bright protrusion chain corresponds to the  $\alpha_R$  chain in the experimental STM images. The zigzag In adatom chain also modulates the Si step edge structure, but the  $\times 3$  modulation is quite small. The weak  $\times 3$  modulation of the Si step edge structure is consistent with that of the  $\alpha$  chain in the experimental STM images. The weak  $\times 3$  modulation might be because the Si step edge structure is either connected weakly to the zigzag In adatom chain or it is influenced indirectly by the zigzag In adatom chain through the modulated neighboring Si chain.

The In<sub>2</sub> model reproduces most of the features of the experimental STM images, but there is a delicate difference between the experimental and simulated STM images. In the experimental STM images, the  $\beta$  chain consists of two protrusions with different brightness. In contrast, the two protrusions of the C<sub>z1</sub> chain in the simulated STM image have similar intensity. For this reason, the In<sub>2</sub> model was further modified, as shown in figure 4. The modified model is called the In–Si adatom chain model with In coverage of 0.06 ML. In the modified model, the In adatom at the T<sub>4</sub> site is replaced by an Si adatom. The alternative arrangement of the In and Si adatoms reproduces the  $\beta$  chain with the two different protrusions in the experimental STM images, as shown in figure 4. This suggests that the heterogeneous zigzag In–Si chain may be more preferred than the homogeneous zigzag In chain. The  $V_s$  dependence of the simulated STM images was also examined. In the simulated filled-state STM image with a high  $V_s$ , the  $\times 3$  modulation of the step edge structure weakens and the zigzag In–Si chain becomes brighter. In the simulated empty-state STM images, the protrusion at the T<sub>4</sub> site decreases with increasing  $V_s$ . This is compatible with the fact that one of the two different protrusions of the  $\beta$  chain in the experimental STM images loses its intensity at a high  $V_s$ .

To determine the relative stability of the atomic structure models, the formation energies of the atomic structure models were calculated as a function of In chemical potential, as shown in figure 5 [40]. Here,  $\Delta\mu_{\text{In}}$  is the relative In chemical potential to the bulk In chemical potential and  $\Delta E_{\text{form}}$  is the relative formation energy to the formation energy of the relaxed bulk-terminated Si(557)-1  $\times$  1 surface [40]. First, the formation energy of the In<sub>7</sub> model was much higher than the formation energy of the Si(557) surface in the whole range of  $\Delta\mu_{\text{In}}$ , which indicates that the In<sub>7</sub> model is not stable. Below  $\Delta\mu_{\text{In}} = -0.48$  eV, the In–Si adatom chain model was the most stable, while the most stable structure above  $\Delta\mu_{\text{In}} = -0.48$  eV was the In<sub>4</sub> model. The energetics suggests that the In–Si adatom chain and In<sub>4</sub> models are the most stable

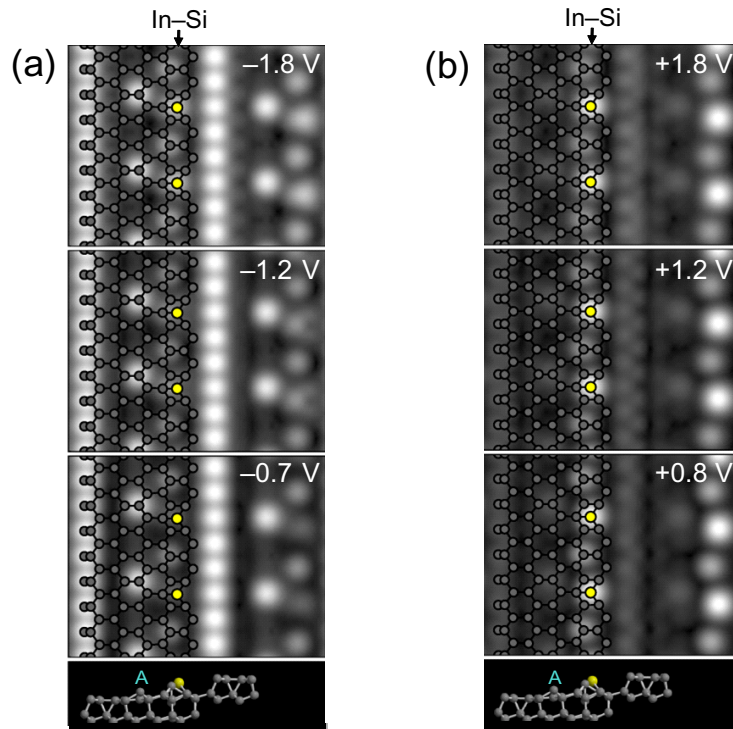


**Figure 4.** The simulated (a) filled- and (b) empty-state STM images of the In-Si adatom chain model.  $V_s$  is written in each image and the atomic structure model is drawn at the bottom. The yellow and gray solid circles denote In and Si atoms, respectively. The raised Si atom in the atomic structure model is denoted by A.

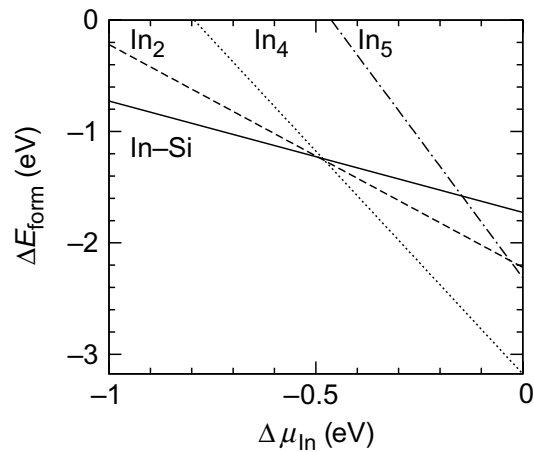


**Figure 5.** The relative formation energies  $\Delta E_{\text{form}}$  of the atomic structure models as a function of the relative chemical potential  $\Delta\mu_{\text{In}}$ . Solid, dashed, dotted and dot-dashed lines denote the  $\Delta E_{\text{form}}$  of the In-Si adatom chain,  $\text{In}_2$ ,  $\text{In}_4$  and  $\text{In}_5$  models, respectively. The  $\Delta E_{\text{form}}$  of the  $\text{In}_7$  model was much higher than zero when  $-1.0 \text{ eV} < \Delta\mu_{\text{In}} < 0 \text{ eV}$ .

at low and high In coverage, respectively. Since the In/Si(557)- $1 \times 3$  surface was observed at low In coverage, the In–Si adatom chain model is more appropriate for the atomic structure model of the In/Si(557)- $1 \times 3$  surface. There is another important result that the In<sub>2</sub> model has the second-lowest formation energy below  $\Delta\mu_{\text{In}} = -0.48$  eV. The formation energy difference between the In<sub>2</sub> and In–Si adatom chain models becomes smaller with increasing  $\Delta\mu_{\text{In}}$  up to  $-0.48$  eV. The small formation energy difference suggests that the In<sub>2</sub> structure could be formed locally on the In/Si(557)- $1 \times 3$  surface at low In coverage. As shown in the experimental empty-state STM image with  $V_s = +1.4$  V (figure 2(b)), bright zigzag chains with the same brightness were observed locally, which is analogous to the simulated empty-state STM image of the In<sub>2</sub> model (figure 3(d)). In addition, the instability of the In<sub>7</sub> and In<sub>5</sub> models implies that an In atom does not prefer the step edge adsorption site. In other words, the instability suggests that the step edge of the In/Si(557)- $1 \times 3$  surface, which produces the  $\alpha$  chain in the experimental STM images, is made out of Si atoms and could produce similar STM images to the  $\times 1$  chain of the Au/Si(557)- $1 \times 2$  surface [15, 31, 32].

The simulated STM images and energetics lead to the conclusion that the In–Si adatom chain model is close to the underlying structure of the experimental STM images. Furthermore, In coverage of the In–Si adatom chain model matches well with the experimental In coverage. This suggests that In and Si adatoms could form an interesting 1D heterogeneous zigzag chain on an Si(557) surface. The interest is further amplified because the arrangement is quite different from the counterpart on an Si(111) surface, the In/Si(111)- $\sqrt{3} \times \sqrt{3}$  surface [37, 38]. The In adatom occupies the H<sub>3</sub> site in the model, while an In adatom is located at the T<sub>4</sub> site on the In/Si(111)- $\sqrt{3} \times \sqrt{3}$  surface [37, 38]. The different adsorption sites may be due to energetic competition between the In and Si adatoms because an Si adatom on the Au/Si(557)- $1 \times 2$  surface also prefers a T<sub>4</sub> site [32]. In addition, the surface total energy of another In–Si adatom chain model with In and Si adatoms at the T<sub>4</sub> and H<sub>3</sub> sites, respectively, was  $\sim 1.0$  eV (unit cell)<sup>−1</sup> higher than the model with In and Si adatoms at the H<sub>3</sub> and T<sub>4</sub> sites, respectively. This suggests that the In–Si adatom chain model with In and Si adatoms at the H<sub>3</sub> and T<sub>4</sub> sites, respectively, is more preferred energetically.

#### 4. Conclusions

The In-induced atomic wires on the Si(557) surface were investigated by STM and first principles calculations. Triple-period atomic wires along the step edge direction were observed at low In coverage by STM. At a high  $V_s$ , the ( $1 \times 3$ ) phase showed a  $\times 1$  straight chain ( $\alpha$ ) in a filled-state STM image and a  $\times 3$  protrusion chain ( $\beta$ ) in an empty-state STM image. At a low  $V_s$ , the  $\alpha$  chain was weakly modulated with  $\times 3$  periodicity, while the  $\beta$  chain was imaged as a zigzag chain. Five atomic structure models based on the atomic structure of the In/Si(111)- $\sqrt{3} \times \sqrt{3}$  surface were examined. Among the candidates, only the In–Si adatom chain model reproduced most of the features of the experimental STM images. In addition, the formation energy of the In–Si adatom chain model was the lowest at low In coverage. In the In–Si adatom chain model, In and Si adatoms are located alternately at the H<sub>3</sub> and T<sub>4</sub> sites along the step edge direction. The  $\alpha$  and  $\beta$  chains in the experimental STM images were interpreted to originate from the weakly modulated Si step edge structure and heterogeneous In–Si adatom chain, respectively.

## Acknowledgments

This study was supported by the Korea Research Foundation Grant funded by the Korean Government (MOEHRD) (KRF-2006-312-C00120) and (KRF-2008-005-J00702) and Korea Science Foundation through the SRC program (Center for Nanotubes and Nanostructured Composites) of MOST/KOSEF.

## References

- [1] Yeom H W *et al* 1999 *Phys. Rev. Lett.* **82** 4898
- [2] Lee S S, Ahn J R, Kim N D, Min J H, Hwang C G, Chung J W, Yeom H W, Ryjkov S V and Hasegawa S 2002 *Phys. Rev. Lett.* **88** 196401
- [3] Kanagawa T, Hobarra R, Matsuda I, Tanikawa T, Natori A and Hasegawa S 2003 *Phys. Rev. Lett.* **91** 036805
- [4] Ahn J R, Byun J H, Koh H, Rotenberg E, Kevan S D and Yeom H W 2004 *Phys. Rev. Lett.* **93** 106401
- [5] Guo J, Lee G and Plummer E W 2005 *Phys. Rev. Lett.* **95** 046102
- [6] Park S J, Yeom H W, Ahn J R and Lyo I-W 2005 *Phys. Rev. Lett.* **95** 126102
- [7] Losio R, Altmann K N and Himpfel F J 2000 *Phys. Rev. Lett.* **85** 808
- [8] Erwin S C 2003 *Phys. Rev. Lett.* **91** 206101
- [9] Yoon H S, Park S J, Lee J E, Whang C N and Lyo I-W 2004 *Phys. Rev. Lett.* **92** 096801
- [10] Kang P-G, Jeong H and Yeom H W 2008 *Phys. Rev. Lett.* **100** 146103
- [11] Choi W H, Kang P G, Ryang K D and Yeom H W 2008 *Phys. Rev. Lett.* **100** 126801
- [12] Erwin S C and Weitering H H 1998 *Phys. Rev. Lett.* **81** 2296
- [13] Ahn J R, Kim N D, Lee S S, Lee K D, Yu B D, Heon D, Kong K and Chung J W 2002 *Europhys. Lett.* **57** 859
- [14] Losio R, Altmann K N, Kirakosian A, Lin J-L, Petrovykh D Y and Himpfel F J 2001 *Phys. Rev. Lett.* **86** 4632
- [15] Ahn J R, Yeom H W, Yoon H S and Lyo I-W 2003 *Phys. Rev. Lett.* **91** 196403
- [16] Nagao T, Yaginuma S, Inaoka T and Sakurai T 2006 *Phys. Rev. Lett.* **97** 116802
- [17] Crain J N, Kirakosian A, Altmann K N, Bromberger C, Erwin S C, McChesney J L, Lin J-L and Himpfel F J 2003 *Phys. Rev. Lett.* **90** 176805
- [18] Ahn J R, Kang P G, Ryang K D and Yeom H W 2005 *Phys. Rev. Lett.* **95** 196402
- [19] Crain J N and Pierce D T 2005 *Science* **307** 703
- [20] Snijders P C, Rogge S and Weitering H H 2006 *Phys. Rev. Lett.* **96** 076801
- [21] Barke I, Zheng F, Rugheimer T K and Himpfel F J 2006 *Phys. Rev. Lett.* **97** 226405
- [22] Tegenkamp C, Kallassy Z, Pfnur H, Gunter H-L, Zielasek V and Henzler M 2005 *Phys. Rev. Lett.* **95** 176804
- [23] Kim K S, Morikawa H, Choi W H and Yeom H W 2007 *Phys. Rev. Lett.* **99** 196804
- [24] Tegenkamp C, Ohta T, McChesney J L, Dil H, Rotenberg E, Pfnur H and Horn K 2008 *Phys. Rev. Lett.* **100** 076802
- [25] Oh D-H, Kim M K, Nam J H, Song I, Park C-Y, Woo S H, Hwang H-N, Hwang C C and Ahn J R 2008 *Phys. Rev. B* **77** 155430
- [26] Kirakosian A, Bennewitz R, Crain J N, Fauster T, Lin J-L, Petrovykh D Y and Himpfel F J 2001 *Appl. Phys. Lett.* **79** 1608
- [27] Kresse G and Hafner J 1993 *Phys. Rev. B* **47** 558
- [28] Perdew J P and Zunger A 1981 *Phys. Rev. B* **23** 5048
- [29] Blöchl P E 1994 *Phys. Rev. B* **50** 17953  
Kresse G and Joubert D 1999 *Phys. Rev. B* **59** 1758

- [30] Tersoff J and Hamann D R 1985 *Phys. Rev. B* **31** 805
- [31] Crain J N, McChesney J L, Zheng F, Gallagher M C, Snijders P C, Bissen M, Gundelach C, Erwin S C and Himpsel F J 2004 *Phys. Rev. B* **69** 125401
- [32] Yeom H W, Ahn J R, Yoon H S, Lyo I-W, Jeong H and Jeong S 2005 *Phys. Rev. B* **72** 035323
- [33] Zhang H M, Balasubramanian T and Uhrberg R I G 2001 *Phys. Rev. B* **65** 035314
- [34] Kawaji M, Baba S and Kinbara A 1979 *Appl. Phys. Lett.* **34** 748
- [35] Lifshits V G, Saranin V G and Zotov A V 1994 *Surface Phases on Silicon* (New York: Wiley)
- [36] Kraft J, Ramsey M G and Netzer F P 1997 *Phys. Rev. B* **55** 5384
- [37] Nicholls J M, Maartensson P, Hansson G V and Northrup J E 1985 *Phys. Rev. B* **32** 1333
- [38] Nicholls J M, Reihl B and Northrup J E 1987 *Phys. Rev. B* **35** 4137
- [39] Saranin A A, Zotov A V, Numata T, Kubo O, Katayama M, Oura K, Ignatovich K V and Lifshits V G 1997 *Surf. Sci.* **388** 299
- [40] Northrup J E 1991 *Phys. Rev. B* **44** 1419